Scaling laws at nonlinear Schrödinger defect sites

Paul K. Newton and Mike O'Connor
Department of Aerospace Engineering, University of Southern California, Los Angeles, California 90089-1191
(Received 6 September 1995)

A new family of defect solutions to the nonlinear Schrödinger equation is described. The defects have standing wave dynamics with j concentric rings centered at the defect site $r=0$, and a conical shape as $r\to 0$ with angle of opening ϕ_j. Using a phase space technique, solution trajectories having a prescribed number (j) of rings are computed along with their corresponding eigenvalue ν_j, and angle of opening ϕ_j. As in the linear Sturm-Liouville theory, the eigenvalues are ordered so that $\nu_{j-1}<\nu_j<\nu_{j+1}$, a fact which is clearly seen from the phase space structure. The nonlinear eigenfunctions are trajectories which lie on the basin boundary between the domains of the attraction of the two asymptotically stable trajectories in the three dimensional phase space. The asymptotic distribution of the eigenvalues for large j, and the angle of opening at the defect site are both shown to have a power law form, and formulas for the power law exponents are given.

PACS number(s): 47.35.+i, 47.20.Ky, 83.10.Ji

I. INTRODUCTION

Defect solutions to nonlinear partial differential equations arise in several physical contexts, including liquid crystals [1], oceanography [2], transitional flows in fluids [3,4], such as shear layers [5], surface wave patterns [2,6–9], and in a wide range of general pattern forming systems [10]. Their role near onset of instability, as modeled by the generic amplitude equation approach, has been documented, for example, in [6,7,4]. From a mathematical point of view, a defect is a topological singularity [11], which at the defect site ($r=0$) has a vanishing amplitude and undefined phase. Like the point vortex solution to the two dimensional equations of ideal fluid flow, a defect site imposes global structure on both the spatial profile as well as the dynamics of the surrounding field [2,12–15]. In this paper we describe a new family of exact defect solutions to the nonlinear Schrödinger equation (NLS). The defects described have a singularity in the spatial profile at $r=0$ with an angle of opening ϕ_j, a characteristic standing wave frequency λ_j with a set of j concentric rings surrounding the defect site. By viewing the problem as a nonlinear Sturm-Liouville eigenvalue problem, we will describe a scaling theory that arises near the defect site which governs the asymptotic distribution (large j) of the oscillation frequencies λ_j and the angle of opening ϕ_j at the defect site.

Our focus is on the nonlinear Schrödinger (NLS) model in two dimensions with power nonlinearity

$$i\psi_t+\nabla^2\psi-|\psi|^s\psi=0, \tag{1.1}$$

where we write the Laplacian in the polar coordinates

$$\nabla^2\equiv\frac{\partial}{\partial r^2}+\frac{1}{r}\frac{\partial}{\partial r}+\frac{1}{r^2}\frac{\partial^2}{\partial\theta^2}. \tag{1.2}$$

Standing wave "ring defect" solutions are of the form: $\psi=\exp[i(-\lambda t+m\theta+\theta_0)]u(r)$, where $\lambda>0$, $m>0$ (integer valued), θ_0=const which we take as zero without loss of generality. This leads to a nonlinear eigenvalue problem for the spatial structure $u(r)$

$$u''+\frac{1}{r}u'-\frac{m^2}{r^2}u+(\lambda-u^s)u=0, \tag{1.3}$$

$$u\sim\beta r^\rho,\quad r\to 0,\quad \rho>0, \tag{1.4}$$

$$u\sim k,\quad r\to\infty. \tag{1.5}$$

For given values of m and s, there are two eigenvalue parameters (λ,β). The boundary condition at the origin imposes the relationship $\rho=|m|$, while the condition at infinity requires either that $k=0$ (for solutions with $\int|u|^2dr<\infty$), or $k=\lambda^{1/s}$ for solutions with homogeneous spatial structure at infinity. Special solutions, called "ground state defects," have previously been studied by Neu [16], distinguished by the fact that $u(r)$ has no zeroes for $r>0$.

In this paper we describe a more general family of defect solutions which we call standing wave "ring defects," where $u(r)$ has a finite number of zeroes ($j=1,2,3,\ldots$) or nodes, and $k=0$. The distance between the origin and the ith node defines the radius of the ith concentric ring around the origin. As in [17], we will view (1.3) as a nonlinear Sturm-Liouville eigenvalue problem in a three dimensional phase space. In this way we will show that (1.3) has an entire family of standing wave ring defect solutions with a prescribed number of rings (j), each with an oscillation frequency λ_j. Each solution trajectory corresponds to a part of the basin boundary separating the basins of attraction of two asymptotically stable trajectories in the phase space. A numerical "squeezing" method is used to locate these solutions and their eigenvalues to arbitrary accuracy. This is accomplished, as in [17], not by solving for the desired solution, but by solving for two adjacent trajectories which are simple to compute and straddle the solution. By squeezing these trajectories arbitrarily close to each other, the desired solution structure is obtained to arbitrary accuracy. We expect that the techniques outlined here will be useful on related models such as the dissipative Ginzburg-Landau model studied by others [12–15].

First, we rescale (1.3)

$$R=\lambda^\alpha r, \tag{1.6}$$

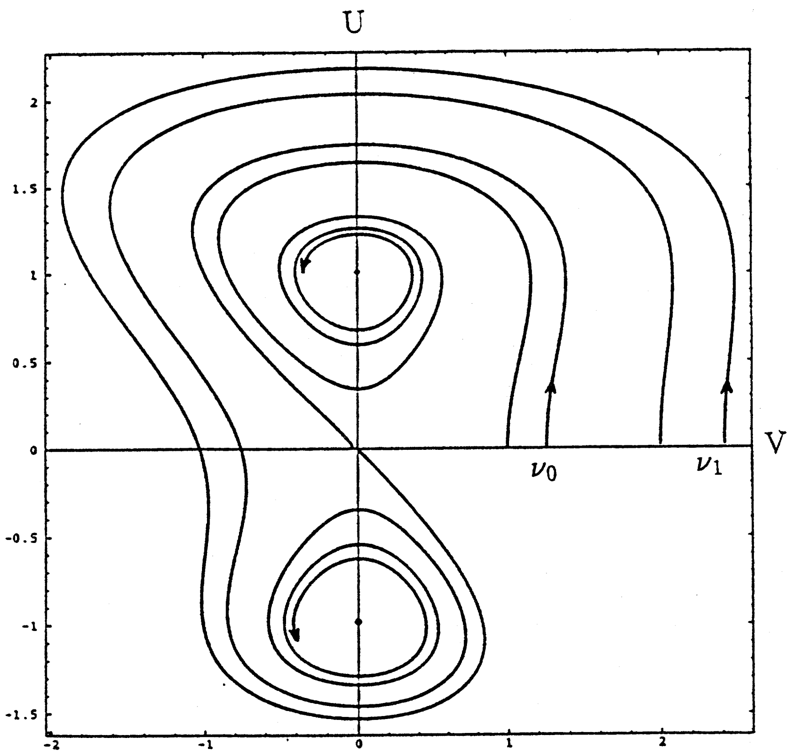

FIG. 1. Projected phase plane (U,V). Trajectories marked ν_0, ν_1 are nonlinear eigenfunctions.

$$U=\lambda^{\gamma}u. \tag{1.7}$$

Then we can eliminate λ from the equations by letting $\alpha=1/2$, $\gamma=-1/s$. This results in the new problem

$$U''+\frac{1}{R}U'-\frac{m^2}{R^2}U-U+U^{s+1}=0, \tag{1.8}$$

$$U\sim \nu R^m, \quad R\rightarrow 0, \tag{1.9}$$

$$U\sim 0, \quad R\rightarrow\infty. \tag{1.10}$$

The rescaled equation has a single eigenvalue parameter ν given by

$$\nu\equiv\frac{\beta}{\lambda^{(2+ms)/2s}}. \tag{1.11}$$

Our focus in this paper is on the case $m=1$, which implies that the defect has a "conical" shape as $R\rightarrow 0$, hence we can define an "angle of opening" at the defect site $R=0$, labeled ϕ_j. We will show that there are discrete values of the eigenvalue parameter $\nu=\nu_j$ and the angle of opening ϕ_j, with $\nu_{j-1}<\nu_j<\nu_{j+1}$, and $\phi_{j-1}<\phi_j<\phi_{j+1}$ where j represents the (integer) number of zeroes of the corresponding eigenfunction $U\equiv U_j$. Using the phase space technique described in Sec. II, we will show that the asymptotic distribution of the eigenvalues ν_j and angles ϕ_j, for large j, follows the power law form. In addition, we propose a power law exponent formula which is consistent with all of the numerical data. To our knowledge, no such power law formulas have been derived for nonlinear Sturm-Liouville problems.

II. PHASE SPACE STRUCTURE

We start by writing (1.8) as a first order system

$$U'=V, \tag{2.1}$$

$$V'=-\frac{V}{W}+\frac{U}{W^2}+U-U^{s+1}, \tag{2.2}$$

$$W'=1, \tag{2.3}$$

with

$$V\sim\nu_j, \quad R\rightarrow 0, \tag{2.4}$$

$$U\sim 0, \quad R\rightarrow\infty. \tag{2.5}$$

In the three dimensional phase space (U,V,W), defect structures satisfying the boundary conditions (2.4), (2.5) are trajectories which start on the V axis for $R=0$, wind around the W axis a prescribed number of times as R increases, then converge to the W axis as $R\rightarrow\infty$. The number of intersections with the V axis ($U=0$) between the starting point and the end point of the trajectory corresponds to the number of zeroes of the eigenfunction.

The defects are most easily viewed projected down to the (U,V) plane, as shown in Fig. 1. On this projected plane, it is easy to prove that as $W\rightarrow\infty$, the system (2.1)–(2.3) has three fixed points $(V,U)=(0,0),(0,\pm1)$. By computing the eigenvalues of the system linearized around each fixed point, as done in [17], we can conclude that:

(1) The fixed points $(0,\pm1)$ are asymptotically stable spirals as $W\rightarrow\infty$.

(2) The fixed point (0,0) is an unstable saddle as $W\rightarrow\infty$.

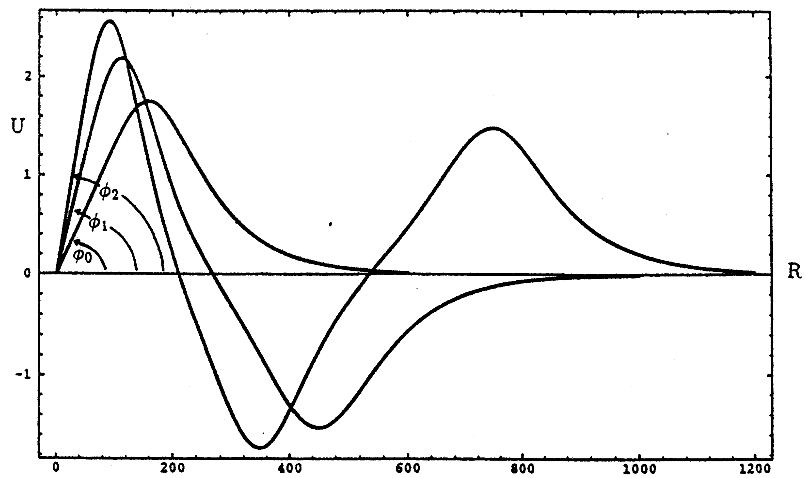

FIG. 2. First three eigenfunctions. Angle of openings ϕ_0, ϕ_1, ϕ_2 corresponding to U_0, U_1, U_2 are marked.

From this structure, as shown in Fig. 1, the technique for computing the eigenvalues ν_j is straightforward. We increase ν along the V axis until the trajectory switches from one converging to the fixed point (0,1) to one converging to the fixed point $(0,-1)$ as $W\rightarrow\infty$. Between the values of ν where the switch occurs lies an eigenvalue. The first eigenvalue, labeled ν_0, is shown in Fig. 1, distinguished by the fact that its trajectory converges to the origin without crossing the V axis. As ν is increased further, the trajectory switches back to (0,1). From this, we can locate the value ν_1 with its corresponding trajectory having one zero. This switching process continues indefinitely as ν is increased, each switch marking a trajectory with one more zero than the previous trajectory.

The following general conclusions can be drawn from this phase space structure:

Proposition:

(1) There exists an infinite number of discrete eigenvalues ν_j linearly ordered such that $\nu_{j-1}<\nu_j<\nu_j+1$. Each integer value j corresponds to the precise number of zeroes of the corresponding nonlinear eigenfunction U_j.

(2) The trajectories converging to the fixed point (0,0) as $W\rightarrow\infty$ are the eigenfunctions of the problem (2.1)–(2.5). They lie on the basin boundary separating the basins of attraction of the two fixed points $(0,\pm 1)$.

(3) The eigenvalue ν_j can be computed to arbitrary accuracy by "squeezing" it between the values $(\nu_j-\epsilon,\nu_j+\epsilon)$ along the V axis. The trajectory with initial data $(U,V)=(0,\nu_j-\epsilon)$ converges to the fixed point $(0,+1)$ if j is even, and $(0,-1)$ if j is odd, with j crossings of the V axis. The trajectory with initial data $(U,V)=(0,\nu_j+\epsilon)$ converges to the fixed point $(0,+1)$ if j is odd, and $(0,-1)$ if j is even, with $j+1$ crossings of the V axis. The eigenvalue ν_j can be located by decreasing ϵ, thereby "squeezing" the true solution between two asymptotically stable trajectories.

(4) Once the eigenvalue ν_j and corresponding eigenfunction U_j is computed, the angular opening at the defect site ϕ_j can be computed via the formula $\phi_j=\tan^{-1}(\nu_j)$. The profile $U_j(r)$ for $j=0$, 1, 2 is shown in Fig. 2, where the angular openings ϕ_0, ϕ_1, ϕ_2 are marked.

III. EIGENVALUES AND POWER LAWS

In Table I we list the computed eigenvalues ν_j for problem (1.8)–(1.10) with $m=1$, for power nonlinearities $s=2$, 4, 6, 8, 10. Even powers of s are chosen so that (1.1) remains invariant under the transformation $\psi\rightarrow-\psi$.

To clearly demonstrate the power law structure in the data, we define

$$f(j)=\frac{\ln[\nu_{j+1}]-\ln[\nu_j]}{\ln[j+1]-\ln[j]}. \tag{3.1}$$

$$g(j)=\nu_j j^{-f(j)}. \tag{3.2}$$

If $\nu_j\sim\alpha j^{\mu}$ as $j\rightarrow\infty$, then $f(j)\rightarrow\mu$ and $g(j)\rightarrow\alpha$. Figures 3 and 4 show plots of $f(j)$ and $g(j)$ vs $1/j$ for the data in Table I. When plotted this way, the y intercept gives the power law

TABLE I. Eigenvalues for various s values.

	$s=2$	$s=4$	$s=6$	$s=8$	$s=10$
ν_0	1.252	1.623	1.911	2.148	2.36
ν_1	2.416	3.675	5.020	6.544	8.27
ν_2	3.572	6.121	9.480	13.883	19.6
ν_3	4.726	8.921	15.230	24.657	38.2
ν_4	5.880	12.036	22.356	39.286	65.9
ν_5	7.033	15.440	30.833	58.150	104.4
ν_6	8.186	19.109	40.661	81.592	155.6
ν_7	9.339	23.027	51.843	109.932	221.2
ν_8	10.492	27.177	64.376	143.473	303.0
ν_9	11.645	31.549	78.263	182.498	402.8
ν_{10}	12.798	36.132	93.503	227.278	522.4
ν_{11}	13.951	40.916	110.096	278.070	663.6
ν_{12}	15.103	45.893	128.042	335.123	828.2
ν_{13}	16.256	51.056	147.341	398.669	1017.9
ν_{14}	17.409	56.399	167.993	468.970	1234.6
ν_{15}	18.561	61.915	189.998	546.180	1480.0
ν_{16}	19.714	67.600	213.357	630.5	1756.0
ν_{17}	20.866	73.448	238.068	722.3	2064.3
ν_{18}	22.019	79.456	264.133	821.6	2406.7
ν_{19}	23.172	85.619	291.551	928.7	
ν_{20}	24.324	91.933	320.323	1043.8	

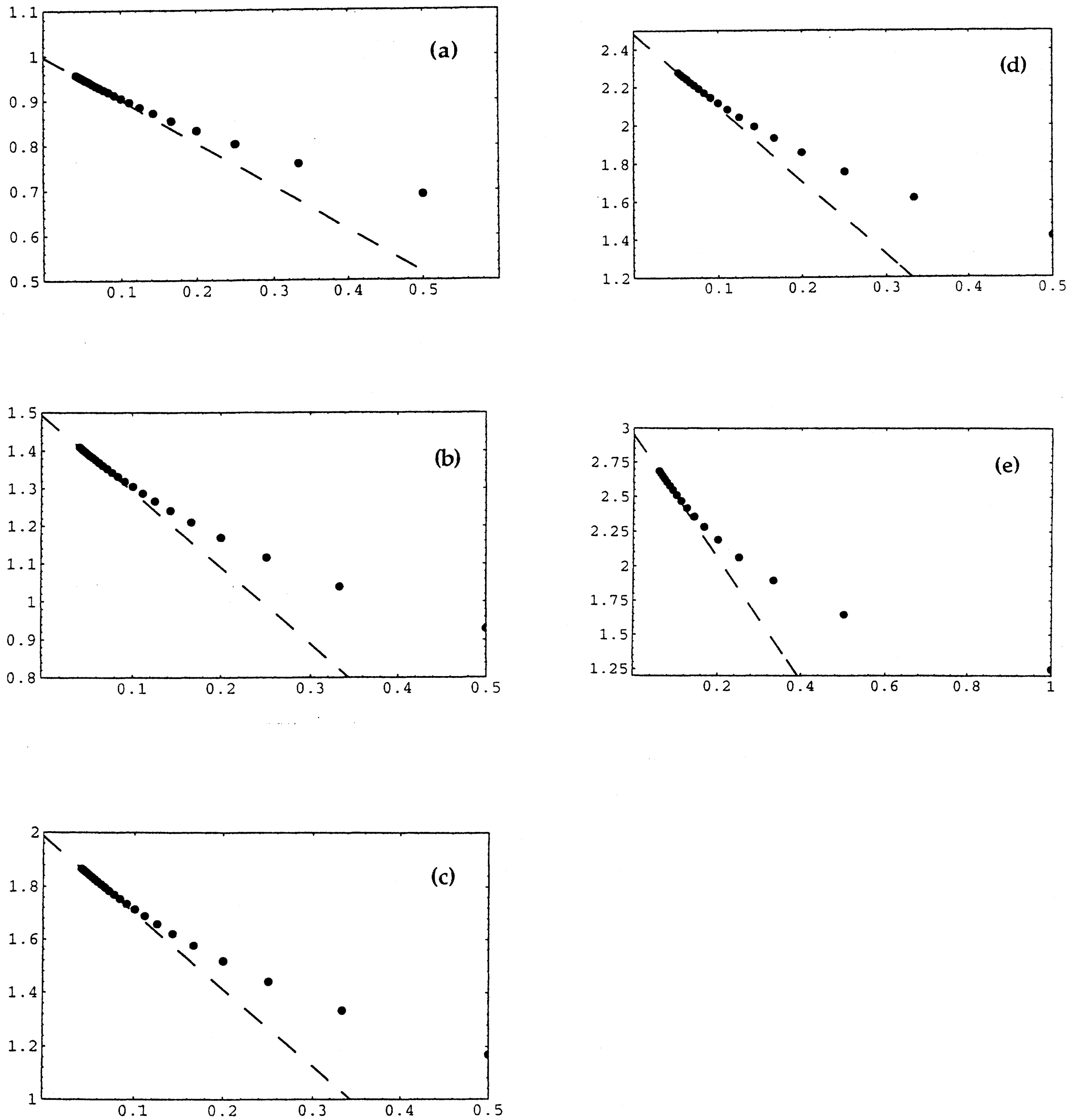

FIG. 3. (a) $f(j)$ vs $1/j$ showing power law form with $\mu=1$, $s=2$. (b) $f(j)$ vs $1/j$ showing power law form with $\mu=1.5$, $s=4$. (c) $f(j)$ vs $1/j$ showing power law form with $\mu=2$, $s=6$. (d) $f(j)$ vs $1/j$ showing power law form with $\mu=2.5$, $s=8$. (e) $f(j)$ vs $1/j$ showing power law form with $\mu=3$, $s=10$.

exponent, μ and power law coefficient α. In each case, we fit a straight line to the last three data points and extrapolate the line to the y axis. The figures reveal the power law exponents and coefficients shown in Table II.

Based on this data, we deduce the simple exponent formula

$$\mu(s)=\frac{2(n-1)}{4-s(n-2)}+\frac{ms}{4}, \tag{3.3}$$

where n is the underlying spatial dimension for (1.1), m is the integer valued winding number, and s is the power of the nonlinearity. For the purposes of this paper we have ($n=2$, $m=1$)

$$\mu(s)=\frac{1}{2}+\frac{s}{4}. \tag{3.4}$$

Formula (3.3) is consistent with the data and formula pro-

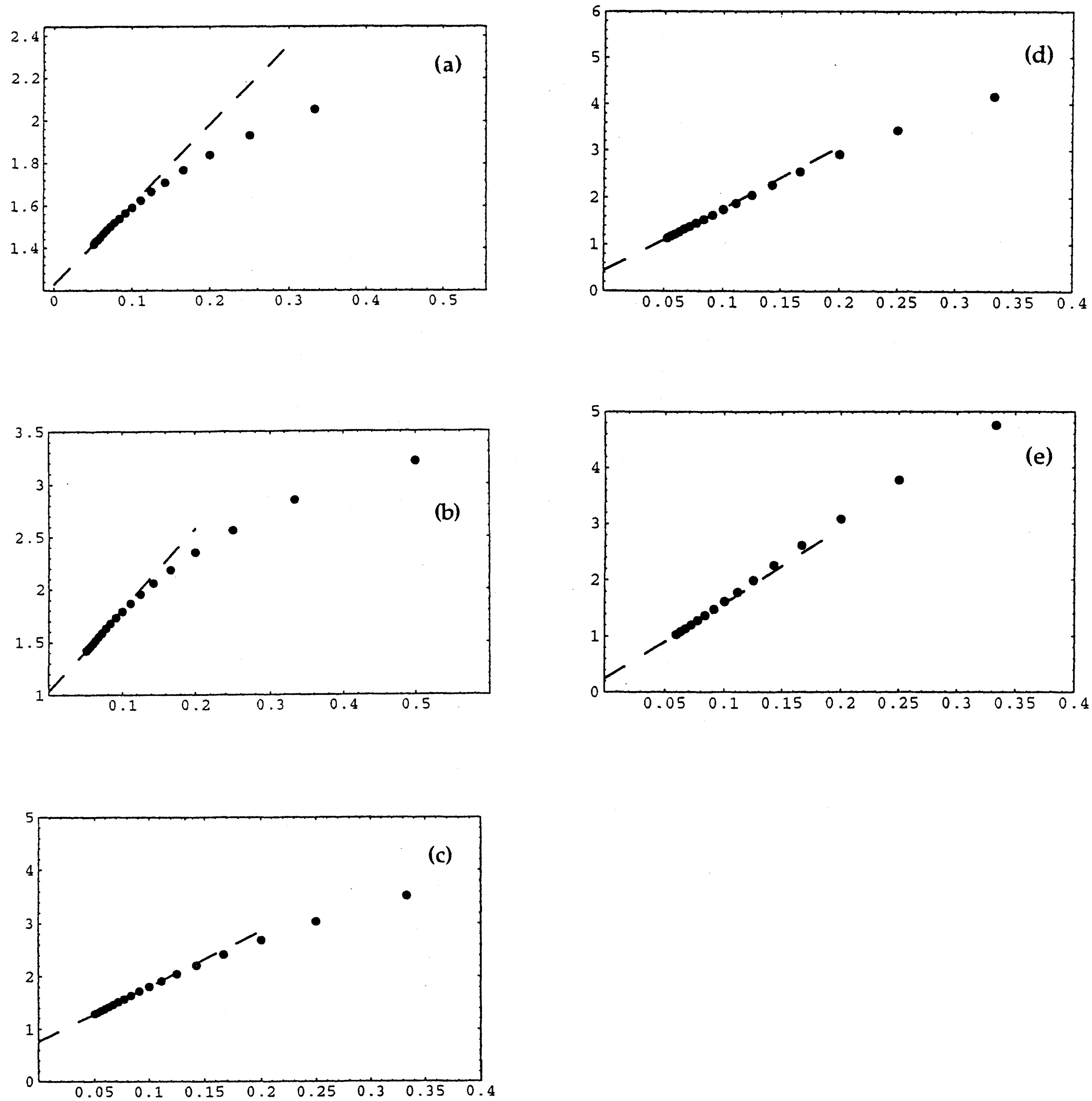

FIG. 4. (a) $g(j)$ vs $1/j$ showing power law form with $\alpha=1.23$, $s=2$. (b) $g(j)$ vs $1/j$ showing power law form with $\alpha=1.03$, $s=4$. (c) $g(j)$ vs $1/j$ showing power law form with $\alpha=0.753$, $s=6$. (d) $g(j)$ vs $1/j$ showing power law form with $\alpha=0.449$, $s=8$. (e) $g(j)$ vs $1/j$ showing power law form with $\alpha=0.241$, $s=10$.

posed in [17] for radially symmetric standing wave solutions to NLS, where $m=0$. While (3.3) is not the *unique* way to generalize the formula of [17], it is the simplest generalization consistent with the data from Table II.

The angle of opening ϕ for $j=0$, 1, 2 is shown in Fig. 2. As mentioned previously, it is related to ν_j via the formula

$$\phi_j=\tan^{-1}(\nu_j). \tag{3.5}$$

TABLE II. Power-law exponent and coefficient for various s values.

$s=2$	$\mu=1.00094(\sim 1)$	$\alpha=1.23$
$s=4$	$\mu=1.49688(\sim 1.5)$	$\alpha=1.03$
$s=6$	$\mu=1.98717(\sim 2)$	$\alpha=0.753$
$s=8$	$\mu=2.48156(\sim 2.5)$	$\alpha=0.449$
$s=10$	$\mu=2.94644(\sim 3)$	$\alpha=0.241$

TABLE III. Comparison of exact vs asymptotic angle of opening.

		$s=2$	$s=4$	$s=6$	$s=8$	$s=10$
$j=5$	exact	1.430	1.506	1.538	1.554	1.561
	asymp	1.408	1.484	1.518	1.531	1.538
$j=10$	exact	1.493	1.543	1.560	1.566	1.569
	asymp	1.490	1.540	1.558	1.564	1.567
$j=15$	exact	1.517	1.555	1.566	1.569	1.5701
	asymp	1.5166	1.554	1.565	1.568	1.5696

For $|\nu_j|>1$ we can use the asymptotic expansion [18]:

$$\phi_j=\tan^{-1}(\nu_j)\sim\frac{\pi}{2}-\frac{1}{\nu_j}+O(1/\nu_j^3), \tag{3.6}$$

along with (3.4) to get the result

$$\phi_j\sim\frac{\pi}{2}-\frac{1}{\alpha}j^{-(1/2+s/4)}. \tag{3.7}$$

In Table III we compare the asymptotic and exact angle of opening for the cases $s=2$, 4, 6, 8, 10, where $j=5,10,15$. As can be seen, the asymptotic formula (3.7) is quite good and improves as j gets large.

IV. DISCUSSION

The power law formulas described here are reminiscent of certain well known features from the classical linear Sturm-Liouville theory. If one solves the Dirichlet eigenvalue problem on an arbitrary domain of length l, area A, or volume V, the asymptotic eigenvalue distribution is known to be governed by the power law formulas [19]:

$$\lambda_j\sim\left(\frac{\pi}{l}\right)^2 j^2, \tag{4.1}$$

$$\lambda_j\sim\left(\frac{4\pi}{A}\right)j, \tag{4.2}$$

$$\lambda_j\sim\left(\frac{6\pi^2}{V}\right)^{2/3} j^{2/3}. \tag{4.3}$$

To our knowledge, these formulas have never been generalized to nonlinear problems, and the results in this paper represent a step in that direction.

A separate issue, outside the scope of this paper, is the question of the stability of these solutions with respect to small perturbations. While there are no results in this direction, we would anticipate, based on the related models, that the defect solutions with j concentric rings with $j>1$ would be unstable dynamically.

ACKNOWLEDGMENTS

This work is supported by a grant from the Office of Naval Research, and the National Science Foundation. The first author (P.K.N.) has profited from many discussions with F. Browand and G. Spedding.

[1] Y. Bouligand, in *Physics of Defects*, Les Houches Session XXXV, edited by R. Balian, M. Kléman, and J. P. Poirier (North-Holland, Amsterdam, 1981).
[2] M. Berry, in *Physics of Defects*, Les Houches Session XXXV, edited by R. Balian, M. Kléman, and J. P. Poirier (North-Holland, Amsterdam, 1981).
[3] L. Gil, J. Lega, and J. L. Meunier, Phys. Rev. A **41**, 1138 (1990).
[4] G. Goren, I. Procaccia, S. Rasenat, and V. Steinberg, Phys. Rev. Lett. **63**, 1237 (1989).
[5] T. Dallard and F. K. Browand, J. Fluid Mech. **247**, 339 (1993).
[6] P. Coullet, C. Elphick, L. Gil, and J. Lega, Phys. Rev. Lett. **59**, 884 (1987).
[7] P. Coullet, L. Gil, and J. Lega, Phys. Rev. Lett. **62**, 1619 (1989).
[8] P. Coullet and J. Lega, Europhys. Lett. **7**, 511 (1988).
[9] G. R. Spedding, F. K. Browand, N. E Huang, and S. R. Long, Dyn. Atmos. Oceans **20**, 55 (1993).
[10] E. Bodenschatz, W. Pesch, and L. Kramer, Physica D **32**, 135 (1988).
[11] N. D. Mermin, Rev. Mod. Phys. **51**, 591 (1979).
[12] L. Pismen and J. Rubinstein, Physica D **47**, 353 (1991).
[13] L. Pismen and J. Rodriguez, Phys. Rev. A **42**, 2471 (1990).
[14] J. Rodriguez, L. Pismen, and L. Sirovich, Phys. Rev. A **44**, 7980 (1991).
[15] H. Sakaguchi, Prog. Theor. Phys. **82**, 7 (1989).
[16] J. C. Neu, Physica D **43**, 385 (1990).
[17] P. K. Newton and S. Watanabe, Physica D **67**, 19 (1993).
[18] *Handbook of Mathematical Functions*, edited by M. Abramowitz and I. A. Stegun (Dover, New York, 1965).
[19] R. Courant and D. Hilbert, *Methods of Mathematical Physics* (Springer, New York, 1937), Vol. II.